Calculated magnetic properties of binary alloys between Fe, Co, Ni, and Cu

P. James
Condensed Matter Theory Group, Physics Department, Uppsala University, S-75121 Uppsala, Sweden

O. Eriksson
Condensed Matter Theory Group, Physics Department, Uppsala University, S-75121 Uppsala, Sweden
and Theoretical Division and Center for Materials Science, Los Alamos National Laboratory, Los Alamos, New Mexico 87545

B. Johansson and I. A. Abrikosov
Condensed Matter Theory Group, Physics Department, Uppsala University, S-75121 Uppsala, Sweden
(Received 11 May 1998)

We present a detailed theoretical investigation of the magnetic properties of all the binary alloys between the 3*d* elements Fe, Co, Ni, and Cu, in the fcc, bcc, and hcp structures using the coherent-potential approximation in combination with a linear muffin-tin orbitals basis set. We consider random, ordered, and partially ordered alloys. Theory is shown to successfully reproduce the magnetic properties of these alloys, and allows an understanding of the physics of the formation of magnetic moments in these systems. We have investigated the correlation between magnetism and local chemical and magnetical surrounding, and find that Fe and Ni display rather different behavior. Our study shows that there is an alloy-induced high-spin–low-spin magnetic phase transition in all Fe-based fcc and hcp alloys. The limitations of a collinear spin model and the Weiss model for explaining the Invar effect are discussed on basis of noncollinear calculations for fcc Fe.
[S0163-1829(98)03146-4]

I. INTRODUCTION

Properties of magnetic materials have always been a subject of great scientific and practical interest. An enormous amount of experimental and theoretical investigations have been carried out to get a deeper understanding of the nature of magnetism in solids.[1] Until recently the possibilities for theory to predict the properties of magnetic alloys, and even pure metals, were very limited, and mainly restricted by applications of simple models. But the situation changed when the density-functional theory and the local-spin-density approximation (LSDA) were formulated,[2–4] and efficient techniques for electronic structure calculations were developed.[5,6] Nowadays the calculations of the standard ferromagnetic (FM) moment of, for example, a transition-metal element, is a routine procedure, and theoretical treatments of increasingly complex problems, such as noncollinear spin configurations,[7,8] spin dynamics,[9] etc., have been made possible.

Though the progress in the abilities to deal with magnetic systems is very impressive, the amount of information obtained so far from first-principles studies is still restricted to mainly ideally periodic solids. There were also numerous investigations devoted to the properties of more complicated systems, as for instance, surfaces of magnetic metals,[10–12] magnetic impurities,[13–17] or disordered magnetic alloys.[18–27] In most applications the main result consists of the calculation of the magnetic moments for the corresponding system. However, it has also been established that in alloys the magnetic properties, ground-state thermodynamic properties, structural and phase stabilities are strongly related to each other and sometimes even in a very unusual and unexpected manner,[23,24,26,28] the most famous example being the Invar effect.[29,30]

Concerning the magnetic properties of binary transition-metal alloys the most relevant experimental information is contained in the so-called Slater-Pauling curve showing a linear increase of the average magnetic moment for early transition-metal alloys when plotted as a function of the increasing electron per atom ratio, followed by a linear decrease of the moments when the average *d* occupation increases for the latter transition-metal alloys, with a maximum for an average *d* occupation situated close to iron. However, some very interesting exceptions from this rule are known to exist. For instance, the magnetic moment of the fcc FeNi alloys is zero over a concentration interval of Fe between 100 and 75%. The same type of quenched moment has been observed in the fcc FeCo alloy, artificially fabricated by precipitation in a Cu matrix.[31] In general, the possibilities to investigate experimentally the magnetic properties of transition-metal alloys as a function of structure, lattice parameter or degree of chemical order are very limited which in turn limits the available data base for a complete coverage of the phenomena.

A possible solution to this problem is provided by first-principles theory, since there are no limitations for the treatment of the metastable, or even unstable phases, provided adequate approximations and reliable techniques are employed. In this paper we present results of a systematic study of magnetic properties of binary alloys between Fe, Co, Ni, and Cu in all possible combinations, and for the three most common close-packed crystal structures; face-centered cubic (fcc), body-centered cubic (bcc), and hexagonal close-packed (hcp). We have also varied the lattice parameters over a wide interval, and have changed the degree of order in the alloys.

We will present our results in a commonly used form, i.e., as a function of the average electron per atom ratio, thereby making it clear where energy band-filling effects play a dominant role, and where the deviations are important.

We will first analyze the behavior of the average magnetic moment in random alloys, how it is formed, and how it dies off as a function of increasing average $3d$-band occupation. The influence of the crystal structure on the magnetic moments will also be discussed, as well as the influence of the ordering effects on the magnetism.

II. METHOD OF CALCULATION

We have used the linear-muffin-tin-orbital (LMTO) method of Andersen and co-workers[6,32–34] in the atomic-sphere, scalar-relativistic, and soft-core approximations. The basis set included s,p, and d orbitals only. Disorder was treated by means of the multisublattice generalization of the coherent-potential approximation (CPA), and relevant details for the present implementation of the LMTO-CPA method can be found in Refs. 35,36. In addition, some calculations for the random fcc FeNi and FeCo alloys have been carried out for a 144 atom supercell using the locally self-consistent Green's function (LSGF) method of Abrikosov *et al.*[37,38] which computationally scales linearly with increasing number of atoms in the system. The supercell has been constructed in such a way that pair-correlation functions for the first six shells are zero, as is the case in a real random alloy. The local interaction zone (LIZ) of the LSGF calculations includes two shells of nearest neighbors (totally 19 atoms), and the calculations are fully converged with respect to the LIZ size both for the total energy and magnetic moments in these systems. The LSGF calculations have been performed for a single Wigner-Seitz radius $R_{WS}=2.633$ a.u.

In this work we employed the Vosko-Wilk-Nusair parametrization[39] for the exchange-correlation energy density and potential. The integration in the reciprocal space has been carried out using 240, 280, and 225 k points in the irreducible parts of the fcc, bcc, and hcp Brillouin zones, respectively. By minimizing the total energy calculated for several Wigner-Seitz radii the equilibrium volume and magnetic moments were found.

Moreover, to improve on the accuracy we used the fixed spin moment method[40] for those alloys where the ferromagnetic (FM) and the paramagnetic (PM) solutions are close in energy. In our calculations we have only considered the parallel spin alignment, no more complicated magnetic configurations (antiferromagnetic, local moment disorder, noncollinear, etc.) have been investigated, except for the case of supercell calculations, discussed in Sec. VI, and for the case of pure fcc Fe, discussed in Sec. VII.

III. CONCENTRATION DEPENDENCE OF AVERAGE MAGNETIC MOMENT

In Fig. 1 the theoretical and experimental magnetic moments for all binary alloys that can be formed between the four elements Fe, Co, Ni, and Cu are presented as a function of the average number of electrons per atom (bottom scale) or nominal number of minority d-band holes (top scale). For example, the $Co_{50}Ni_{50}$ alloy corresponds to an effective alloy

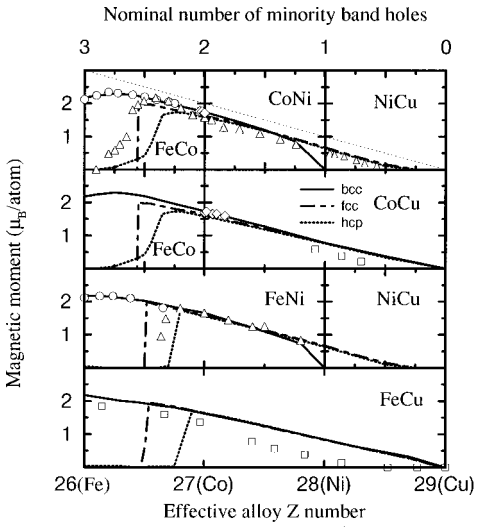

FIG. 1. Average magnetic moment as a function of effective alloy Z number (bottom scale) in random bcc (solid line), fcc (dot-dashed line), and hcp (dotted line) binary alloys between Fe, Co, Ni, and Cu. The graphs are arranged in a scheme that focuses on the influence of the successive filling of the $3d$ band. In order to make a presentation complete the results for the alloys FeCo and NiCu are displayed twice. Experimental results are shown by open circles (bcc alloys), triangles (fcc alloys), diamonds (hcp alloys), and squares (unspecified structure or thin films) (Ref. 31). Experimental results for the mechanically alloyed Fe-Cu system are shown by squares (Ref. 41). The top scale shows a nominal number of minority band holes, and the thin dotted line represents the spin moment of isolated atoms.

Z number 27.5 and d-band hole number 1.5, etc. Graphs are put on top of each other in order to focus on the influence of the fractional d-band filling. To make the presentation complete, two alloys (FeCo and NiCu) have been displayed twice.

The agreement between experiment[31,41] and theory is about as good as calculations based on LSDA normally are for elements and ordered compounds. This illustrates the applicability of our computational technique to the type of problems discussed in the present paper, and allows us to analyze the physical reasons behind the calculated trends. Some deviations between the theoretical and experimental data can be seen for the fcc FeCo and the fcc FeNi alloys at about 26.5 electrons/atom, i.e., in the region where the magnetic moment appears, and for the Cu-rich Co-Cu and Fe-Cu alloys. These deviations will be discussed in Sec. VII.

The first remark we want to make is that the magnetic moment, in a very simple picture, depends weakly on the crystal structure, and decreases almost linearly with an increasing number of electrons. As a matter of fact, this kind of trend is displayed already for the free atoms (if the orbital moment is assumed to be quenched), as shown in the top panel of Fig. 1. This is a clear illustration of the fact that the magnetic moment of $3d$ transition-metal alloys is formed by quite localized d-electron states with a bandwidth of 3–4 eV. This picture, of course, breaks down when one considers the earlier transition-metals and is definitely not sufficient for a deeper understanding of the magnetism of transition metal alloys.

In a crystal the $3d$ levels form a relatively narrow band

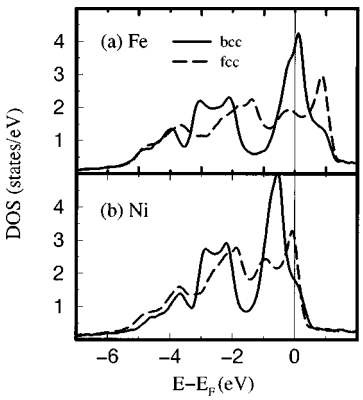

FIG. 2. Density of states (DOS) as a function of energy (relative to the Fermi energy E_F) for the paramagnetic Fe (a) and Ni (b) in the bcc (solid line) and the fcc (dashed line) structures.

due to the hopping of electrons between neighboring atoms. This is an obvious explanation for deviations of the calculated magnetic moments from those of the free atom. As a result the localized electron picture has to be substituted by an itinerant model where the existence of magnetism is related to whether the Stoner criterion is fulfilled or not

$$IN(E_F)>1, \tag{1}$$

where $N(E_F)$ is the alloy density of states (DOS) at the Fermi level (E_F) in the paramagnetic phase, and I denotes the so-called Stoner parameter which is an intra-atomic quantity and is known to depend only little on crystal environment. The Stoner criterion states that ferromagnetism appears when the gain in exchange energy is larger than the loss in kinetic energy. Therefore, there is always a competition between FM and PM solutions, and magnetic properties are determined by the state which has lowest energy.

The Stoner model allows us to understand the structural dependence of the magnetic moment, which is found to be most pronounced in the Fe-rich alloys and for Ni. To be specific, the magnetic moment for pure bcc Fe at the equilibrium volume is $2.18\mu_B$, but zero in the fcc and hcp phases, an effect that Eq. (1) explains. The opposite situation occurs for Ni which in the bcc structure shows an intricate magnetic behavior. A metastable solution with a nonzero magnetic moment is found when the lattice is expanded slightly. But from careful fixed spin moment calculations we predict the nonmagnetic solution to be the stable solution at equilibrium. These results for Fe and Ni are in agreement with earlier studies.[42] In Fig. 2 we show the paramagnetic DOS for Fe and Ni in the fcc and bcc phases at their corresponding equilibrium lattice constants. One finds that the observed structural dependence of the magnetic moment is explained by the difference between the DOS for the bcc and the fcc phases. The bcc DOS has a characteristic structure with two well defined maxima for the bonding and antibonding states, respectively, while the fcc DOS is more uniform as a function of energy. As a result of the filling of these d bands by about 6.5 d electrons in Fe, the Fermi level lies at a peak in the DOS of the bcc phase, resulting in higher density of states compared to the fcc phase. As the Stoner parameter, I in Eq. (1), does not depend on structure, the Stoner criterion is fulfilled for bcc Fe, but not for fcc Fe.

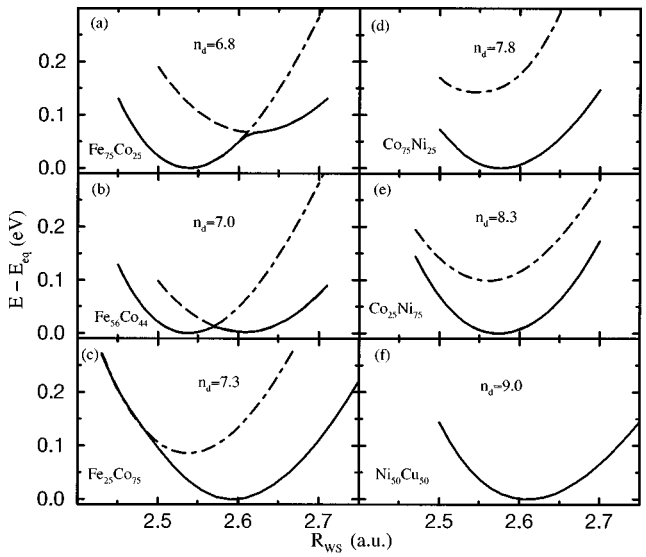

FIG. 3. Evolution of the binding energy curve in the fcc random alloys between $3d$ metals with increasing fractional filling of a d band by $3d$ electrons n_d. Total energy (relative to the equilibrium energy) is shown as a function of Wigner-Seitz radii R_{WS}. Solid drawn lines correspond to the locally stable solutions, the dot-dashed lines show the PM solutions and the dashed lines are extrapolations of the high-spin branches, to volumes where these solutions are not stable even locally.

Because the antibonding peak in the bcc phase is relatively narrow, the opposite situation takes place in Ni when filling the bcc and fcc bands by approximately 8.5 electrons. The Fermi level is now on the other side of the antibonding peak in the bcc phase, and the DOS is higher in the fcc phase. Since band-structure calculations give that the fcc and hcp DOS are quite similar to each other, we find a common behavior for the magnetic moments for these two phases also.

The clear dependence of the average magnetic moment on the effective alloy Z number, seen in Fig. 1, illustrates that it is the filling of the d band which dictates many of the magnetic properties of alloys between transition metals. It also shows the strength of the Stoner model for understanding these phenomena.[43]

In Fig. 3 the existence and the underlying mechanisms of the competition between the PM and the FM solutions are illustrated by showing the evolution of the volume dependence of the binding energy curves for the fcc alloys as the band filling increases. In these graphs it is the fractional filling of the band that is of interest, not the particular alloy chosen. The behavior is also similar for the other structures, and we have chosen fcc as an example. The differences between different structures will be discussed later. Notice that sometimes a solution with a small magnetic moment (the low-spin solution, LS) is more stable than the PM solution. To distinguish this solution from the one with a larger magnetic moment we call the latter the high-spin (HS) state. The total energy relative to its equilibrium value is plotted as a function of Wigner-Seitz radius. The solid line corresponds to the magnetic configuration with the lowest energy. The dot-dashed lines show the PM solutions and the dashed lines are extrapolations of the high-spin branches, to volumes where these solutions are not stable even locally. In the panels (a) and (b) two distinct energy minima are seen corre-

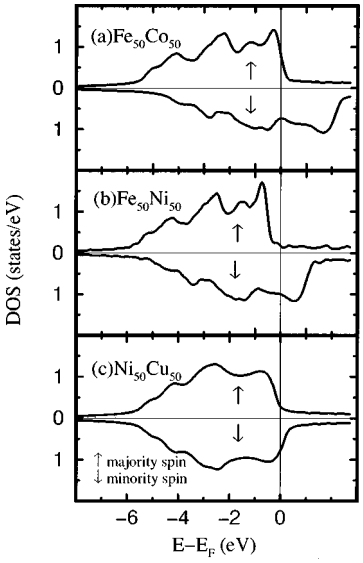

FIG. 4. Spin-resolved density of states (DOS) for random fcc $Fe_{50}X_{50}$ alloys (X=Co, Ni, Cu) as a function of energy (relative to the Fermi energy E_F). The DOS for a majority- and a minority-spin channels are denoted by ↑ and ↓, respectively.

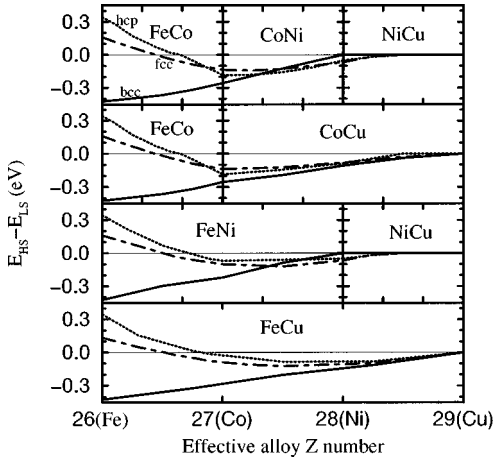

FIG. 5. The energy difference between the high-spin (HS) solution and the low-spin (LS) solution as a function of effective alloy Z number. Notations are the same as in Fig. 1.

sponding to the LS (at lower volumes) and to the HS (at higher volumes) states, respectively. In panel (a) the low-spin state is more stable than the high-spin state. In panel (b), however, one sees a very intricate competition between the two spin states. Careful fixed spin moment calculations had to be performed to resolve the situation. By a slight increase of the amount of d electrons, the high-spin state becomes the stable one. The discontinuous jump in the magnetic moment seen in Fig. 1 is driven by this competition between the high- and the low-spin states. Notice that this discontinuity occurs at practically the same electron concentration (at about 26.5 effective alloy Z number) in all Fe-based alloys. At this particular band filling the total energy for the high-spin and low-spin state happens to be equal [see Fig. 3(b)].

When further increasing the number of d electrons the high-spin state becomes more and more favored [see Fig. 3(c)]. For fcc FeNi the high spin to low spin transition occurs at a Ni concentration of 26%. In this concentration region the system is known, from experiments, to qualify as an Invar system, with zero or very small thermal expansion.[29,30] This was also discussed in Ref. 24. The studies presented here suggest that as a result of the high spin to low spin transition in the fcc and hcp alloys, in combination with an energy competition between these states, the Invar effect would be seen in all close-packed Fe-based alloys. In practice this is not the case because neither the fcc nor the hcp phases of the FeCo and FeCu systems are crystallographically stable.

It is important to point out that at these concentrations the filling of the majority spin channel is almost complete, as shown in Fig. 4(a), where the spin-resolved DOS for the fcc $Fe_{50}Co_{50}$ alloy is shown. When further increasing the amount of $3d$ electrons in the alloy, the minority-spin channel must successively become filled with these electrons. This is manifested in Figs. 4(b) and 4(c) where the DOS for the fcc $Fe_{50}Ni_{50}$ and $Ni_{50}Cu_{50}$ alloys are presented. As a consequence, the average spin moment decreases gradually and the energy difference between high-spin and low-spin states becomes smaller [Figs. 3(d)–3(f)]. Notice, that not only the energy difference between the HS and LS states decreases, but also their equilibrium volumes approach each other. The reason for this is of course the decrease of the magnetic moment, whereby the magnetic expansion of the lattice decreases. Towards the end of the series ($\sim$9–9.5 d electrons), when also the minority spin channel is about to become filled, the high-spin state loses its magnetic moment and the two curves merge gradually. For Cu-rich alloys the magnetic and nonmagnetic curves join completely and the LS and HS states become degenerate.

In Fig. 5 the energy difference between the HS and the LS states is displayed for the three different structures (bcc, fcc, and hcp) as a function of effective alloy Z number (or, equivalently, as a function of the band filling). As discussed earlier, bcc Fe is stable in the HS state, and thereby the solid curves start at large negative values. On the contrary, fcc and hcp Fe are more stable in the LS phase and thereby the dotted and the dot-dashed lines start with positive values. A sharp crossover occurs for these two structures at higher electron concentrations ($Z\sim26.5$ for fcc alloys and $Z\sim26.8$ for hcp alloys) and for higher Z numbers all alloys are more stable in a ferromagnetic phase. For the Cu-rich region all curves merge the zero line. This is directly related to the LS-HS evolution described above. The first crossing corresponds to the case when the HS minimum becomes lower in energy than the LS minimum, and the second crossing occurs when the HS and the LS states become degenerate. One can also see that these curves are almost completely determined by the corresponding band filling, and have characteristic parabolic shape. The later phenomenon has already been discussed in Ref. 24, where the parabolic shape has been explained in the framework of a rectangular DOS model, proposed by Friedel.[44] It is more surprising that this simple model, as well as other band-filling based arguments, works so well in all alloys considered here. We will soon show that partially decomposed DOS deviate substantially from a rigid band behavior. This does, however, not contradict the discussion above in a serious way.

An explanation for why the band-filling arguments still can be used is that the *total* alloy DOS for all alloys really exhibit a behavior similar to the rigid band-type behavior, as

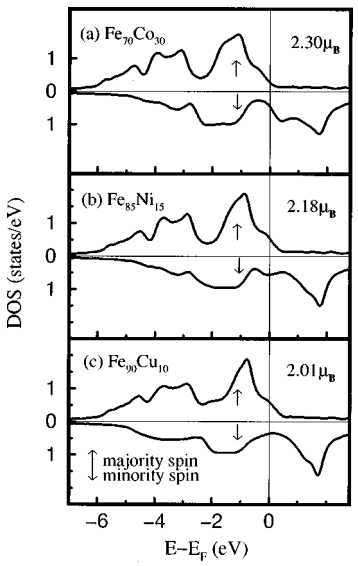

FIG. 6. Spin-resolved density of states (DOS) for random bcc $Fe_{70}Co_{30}$ (a), $Fe_{85}Ni_{15}$ (b), and $Fe_{90}Cu_{10}$ (c) alloy. Notations are the same as in Fig. 4.

can be seen in Fig. 4. This means that the bands first split to give a filled majority band, thereafter only the minority-spin channel is filled when the electron concentration is increased. This is certainly not true for the DOS projected onto atomic spheres of the alloy components which will be discussed later. However, in the total DOS the peculiarities of the individual DOS curves shows up to a much smaller degree, and do not strongly influence properties such as the average magnetic moment of an alloy or the LS-HS energy difference.

Higher-order effects do exist, and are seen, especially for the Cu-rich alloys. For instance, we have calculated, in agreement with experiment, a zero average magnetic moment for Cu-rich CuNi alloys, but finite moments for CuCo and CuFe alloys. The main trends of the average magnetic moment of an alloy, however, are determined by the filling of the alloy *d* band. This is the reason for the successful description of the magnetism in 3*d* alloys in terms of the Slater-Pauling curve.

For FeCo in the bcc structure one can clearly see the characteristic Slater-Pauling behavior of the magnetic moment when varying the concentration of the constituent atoms (Fig. 1). As has been said above, the calculated equilibrium magnetic moment for pure bcc Fe is $2.18\mu_B$. Adding a small fraction of Co causes the moment to increase up to $2.30\mu_B$ for $Fe_{70}Co_{30}$. The maximum at 30% is usually explained by the fact that the Fermi level is pinned in a valley of the minority-spin channel which forces the majority spin channel to saturate [see Fig. 6(a)].[45–47] At 30% concentration of Co this is more or less the case and the magnetic moment gradually decreases when further increasing the amount of Co. When Fe is alloyed with Ni and Cu one would, based on the same band-filling arguments, expect to see the same trend at the same fractional filling, i.e., a maximum magnetic moment at around $Fe_{85}Ni_{15}$ and $Fe_{90}Cu_{10}$. This is, however, not the case. The maximum magnetic moment for these systems is found for pure Fe. Alloying with Ni or Cu decreases the moment and a maximum does not occur. Our results are, in general, in line with the experimental observations. For bcc FeCo containing 20% Co the observed magnetic moment is $0.22\mu_B$ higher than for the pure Fe. For bcc FeNi, with 12% Ni, the experimental magnetic moment is only $0.04\mu_B$ higher than for pure Fe (Ref. 31) whereas our calculations give that the average moment is $0.02\mu_B$ lower. For bcc FeCu the experimental magnetic moment is steadily decreasing when adding more Cu into the alloy, in agreement with our findings. Notice that in the experiments a certain amount of short-range order is always present. Therefore, the small increase of the magnetic moment in bcc FeNi alloy could be related to this.

The above observation is a direct reflection of the fact that the rigid-band model cannot be mechanically applied in all situations. In particular, one can see in Figs. 6(b) and 6(c) that the spin-up band of Fe is not completely filled in $Fe_{85}Ni_{15}$ and $Fe_{90}Cu_{10}$ alloys. The reason behind this is that the DOS of the minority channel of FeCo has a somewhat more pronounced valley at the Fermi level than FeNi and FeCu (see Fig. 6), and this leads to a faster saturation of the majority-spin channel. Therefore, the saturation of the spin-up band, successfully used as an argument in case of the bcc FeCo alloys to explain the maximum at the Slater-Pauling curve, cannot automatically be applied for the bcc FeNi and FeCu. This will be discussed more in the next section.

IV. INDIVIDUAL MAGNETIC MOMENTS

The example above indicates that simple band-filling arguments cannot successfully describe intricate magnetic properties of transition-metal alloys. Significant deviations from the rigid-band model behavior occur as soon as one considers the decomposition of the total moment into the individual contributions from the alloy components. In Figs. 7–9 the individual magnetic moments of the same alloys as in Fig. 1 are displayed. Note that in a real alloy a distribution of the values of the magnetic moments for chemically equivalent atoms with different chemical surrounding is present, as will be discussed later. All values in Figs. 7–9 correspond to the restricted average magnetic moments for alloy components, i.e., magnetic moments averaged over all atoms of the same sort in the alloy. In the framework of the CPA such an averaging is done automatically, and all fluctuations of properties between chemically equivalent atoms are neglected. Recently it has been shown that the CPA provides a very good description of average properties for completely random alloys, but that one must be more careful calculating restricted averages (like the local DOS or individual magnetic moments) within this approximation.[48] Therefore, it is very important to compare our results with experiments as well as with theoretical results obtained by more accurate computational methods, not based on a single-site approximation.

Experimental data are found in Ref. 31 for fcc FeNi and CoNi (Fig. 7) and good agreement with theory is seen. In general, the agreement is comparable with what is seen in Fig. 1 for the average magnetic moments. To compare our results with other first-principles techniques we display in Figs. 7 and 9 available data for magnetic moments of single impurities in corresponding hosts, calculated by the Green's-

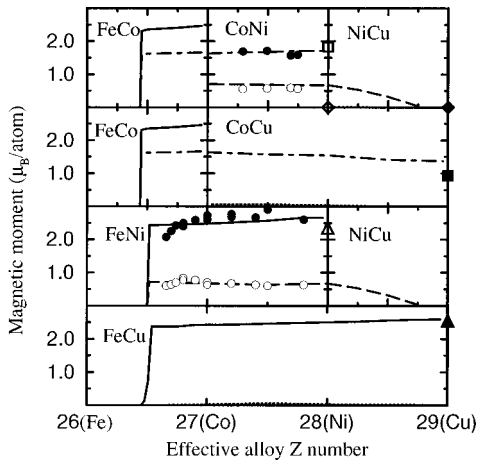

FIG. 7. Average magnetic moments of alloy components as a function of effective alloy Z number in random fcc alloys between Fe, Co, Ni, and Cu. The calculated individual magnetic moments for the Fe are shown by solid lines, for the Co by dot-dashed lines, for the Ni by dashed lines, and for the Cu by dotted lines. Experimental results from Ref. 31 are shown for Co-Ni alloys (by filled circles for the Co and open circles for the Ni) and Fe-Ni alloys (by filled circles for the Fe and open circles for the Ni). Calculated magnetic moments of single impurities of Co in Ni (open square), Cu in Ni (open diamond), Co in Cu (filled square), Ni in Cu (filled diamond), Fe in Ni (open triangle) and Fe in Cu (filled triangle) are taken from Refs. 13,15.

function technique by a number of authors.[13–17] These results agree well with each other, and with our individual moments extrapolated to the impurity limit. As a final test we have performed self-consistent calculations for fcc $Fe_{50}Co_{50}$ and $Fe_{50}Ni_{50}$ alloys modeled by a large supercell of 144 atoms by means of the LSGF method.[37,38] The relevant details is given in Sec. II. Magnetic moments for the FeCo and FeNi alloys calculated by the CPA and the LSGF are given in Table I, and from this table one can clearly see that the CPA gives a reliable description of the total magnetic moments, as well as the magnetic moments averaged over the individual alloy components. The CPA results presented in this paper are thus trustworthy.

From the data presented in Figs. 7–9 we see that the Fe moment in all systems and for all structures increases up to

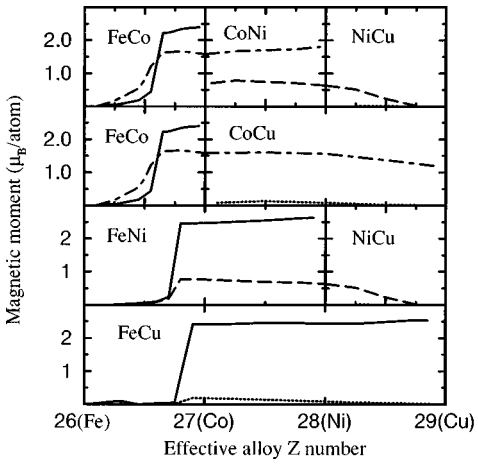

FIG. 8. Same as in Fig. 7 but for the random hcp alloys.

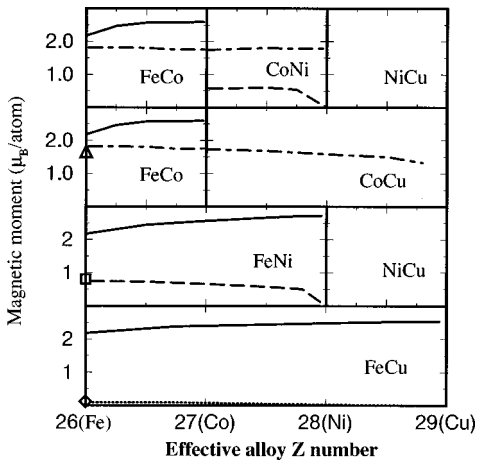

FIG. 9. Same as in Fig. 7 but for the random bcc alloys. Calculated magnetic moments of single impurities of Co in Fe (open triangle), Ni in Fe (open square) and Cu in Fe (open diamond) are taken from Ref. 14.

around $2.5\mu_B$ when it is alloyed with another element. On the other hand, the magnetic moment on Co has a more or less constant value in all alloys. The Ni moment is almost constant when it is alloyed with Fe and Co but its magnitude decreases to zero when it is alloyed with fcc or hcp Cu (the bcc CuNi alloy is paramagnetic). Cu stays almost nonmagnetic for all structures and all alloys. Noticeable is that the structural dependence of the magnetic moments is not very strong. Exceptions are the Fe-rich fcc and hcp alloys where the low-spin to high-spin transition is seen, and the bcc Ni and NiCu alloys which are nonmagnetic.

Slow variations of the individual magnetic moments with concentration of an alloy (except for the LS to the HS transition in the fcc and the hcp Fe-based alloys) are consistent with nearly linear variations of the average magnetic moment. However, one can clearly see that the magnetic moment of Fe in the bcc crystal saturates faster when Co is added to the alloy compared to Ni or Cu. This is in agreement with the densities of states shown in Fig. 6 where the filling of the majority-spin channel for Fe decreases when going from FeCo through FeNi towards the FeCu bcc random alloys with the same total filling of the d band. This somewhat faster increase of the magnetic moment on the Fe site in the bcc FeCo alloy explains the maximum in the average magnetic moment curve (Fig. 1) which appears for FeCo but not for FeNi or FeCu. Next, we use a model similar to one of Ref. 47 and assume a linear increase of the Fe magnetic moment in an Fe-rich alloy, as well as a constant value of the impurity magnetic moment,

TABLE I. Comparison of CPA and supercell LSGF results for average magnetic moments (in Bohr magnetons) in random fcc $Fe_{50}Co_{50}$ and $Fe_{50}Ni_{50}$ alloys ($R_{WS}=2.633$ a.u.).

Method	$Fe_{50}Co_{50}$			$Fe_{50}Ni_{50}$		
	Fe	Co	av.	Fe	Ni	av.
CPA	2.431	1.639	2.035	2.535	0.672	1.604
LSGF	2.436	1.633	2.035	2.535	0.672	1.604

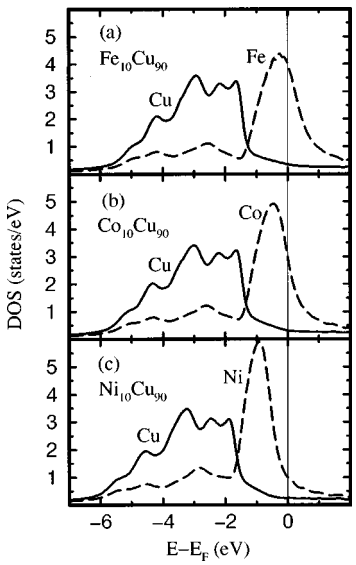

FIG. 10. Density of states (DOS) as a function of energy (relative to the Fermi energy E_F) for the paramagnetic random fcc $Fe_{10}Cu_{90}$ (a), $Co_{10}Cu_{90}$ (b), and $Ni_{10}Cu_{90}$ (c) alloys. Partial DOS of Cu and impurity (Fe, Co or Ni) are shown by full line and by dashed line, respectively.

$$\mu_{\mathrm{Fe}} = \mu'_{\mathrm{Fe}} c + \mu^0_{\mathrm{Fe}}, \qquad \mu_{\mathrm{imp}} = \text{const.} \tag{2}$$

In Eq. (2),

$$\mu'_{\mathrm{Fe}} = \left.\frac{d\mu_{\mathrm{Fe}}}{dc}\right|_{c=0} \tag{3}$$

and c is the concentration of the impurity component (i.e., Co, Ni, or Cu), and μ^0_{Fe} is the magnetic moment of pure bcc Fe. From this it is easy to show that the concentration, $c_{\max}$, at which maximum average magnetic moment occurs is

$$c_{\max} = \frac{1}{2} + \frac{\mu_{\mathrm{imp}} - \mu^0_{\mathrm{Fe}}}{2\mu'_{\mathrm{Fe}}}. \tag{4}$$

The second term in Eq. (4) will always be negative because Fe always has higher magnetic moment than the corresponding impurity. Studying the impurity series Co-Ni-Cu, the value of μ_{imp} successively decreases together with the value of μ'_{Fe} (see Figs. 6 and 7). The decrease of these two factors can move $c_{\max}$ from a point above 0 in the bcc FeCo alloy to a point below 0 in the bcc FeNi and FeCu alloys, as it actually does. This, together with the analysis of the density of states for the corresponding bcc alloys (Fig. 6) presented above, explains the limitations of the rigid-band model predictions for the concentration dependence of the average magnetic moments in different bcc alloys described at the end of Sec. III.

Another very interesting situation occurs in the fcc and the hcp Cu-rich alloys. The local magnetic moment on the Ni vanishes at about 60% of Cu, but local moments on Fe and Co remains nonzero up to the dilute limit. This situation becomes clear when analyzing the paramagnetic local density of states for the alloy components in fcc Cu-rich alloys, presented in Fig. 10. We see that in all cases impurities of transition-metal elements form virtual bond states close to the Fermi level. This means, first of all, that the shape of the DOS for Fe, Co, and Ni changes drastically compared to their elemental DOS. It can be seen that the virtual bond state of Ni is centered *below* the Fermi energy, while, for Fe and Co it is centered *at* the Fermi energy. For the CuNi alloy this situation has been discussed by Tersoff and Falicov[53] who showed on the basis of calculations for stoichiometric NiCu compounds that the possible reason for the filling of the Ni d band and its shifting off the Fermi level should be intra-atomic sp to d electrons charge transfer (charge transfer between Ni and Cu is too small to account for this effect). In Table II the net charges inside the atomic spheres of pure fcc Fe, Co, and Ni, as well as their impurities in Cu are given, where the effect, predicted by Tersoff and Falicov is clearly seen. As Ni has an almost filled d band, this intra-atomic charge transfer is enough to shift the virtual-bound state for the Ni impurity in Cu below the Fermi level and therefore to lower the DOS for Ni atoms below the value which is needed to satisfy the Stoner criterion. Hence, it becomes nonmagnetic. In contrast, the d bands of Co and Fe are too far from being filled, and the charge transfer is too weak to shift their virtual bound states below the Fermi energy. Thus, Fe and Co impurities in Cu should remain magnetic, in agreement with our calculations, earlier impurity calculations as well as experiment.[13,15]

TABLE II. Number of electrons in the atomic spheres of fcc Fe, Co, and Ni.

Element	System	s	p	d	Total
Fe	Pure	0.640	0.807	6.554	8.000
	$Fe_{10}Cu_{90}$	0.591	0.673	6.715	7.978
Co	Pure	0.651	0.800	7.550	9.000
	$Co_{10}Cu_{90}$	0.611	0.695	7.674	8.980
Ni	Pure	0.659	0.749	8.592	10.000
	$Ni_{10}Cu_{90}$	0.655	0.720	8.660	10.036

V. ORDERING AND MAGNETIC MOMENT

In Table III the magnetic moments of the ordered binary alloys between Fe, Co, Ni, and Cu are compared with the magnetic moments of random alloys. We have considered the CsCl (or $B2$) structure as the ordered phase of the bcc underlying lattice, while the CuAu ($L1_0$) structure and Cu_3Au ($L1_2$) structure have been considered as the ordered phases on the fcc underlying lattice. Note that in the $B2$ structure only the compound with equiatomic composition can be perfectly ordered. For the off-stoichiometry compositions partially ordered alloys have been considered with one sublattice fully occupied by the atoms with largest concentration and the other sublattice randomly occupied by the remaining atoms. The ordered alloys on the fcc underlying lattice were considered as completely ordered.

Ordering of the bcc FeCo alloy which is the only stable $B2$ phase among those considered in the present study, increases the moment slightly. This increase of the magnetic moment for FeCo is in very good agreement with magnetization measurements.[31] To pick an example; for $Fe_{50}Co_{50}$ the rise in moment going from a random alloy to an ordered

TABLE III. Theoretical magnetic moments of ordered alloys compared with corresponding random alloys.

		bcc			fcc		
		$x=25$	$x=50$	$x=75$	$x=25$	$x=50$	$x=75$
$Fe_{1-x}Co_x$	Ord	2.30	2.27	2.00	0.0	2.04	1.83
	Rand	2.30	2.20	1.95	0.0	1.97	1.81
$Fe_{1-x}Ni_x$	Ord	2.09	1.73	1.13	1.75	1.64	1.20
	Rand	2.02	1.66	1.09	0.0	1.58	1.15
$Fe_{1-x}Cu_x$	Ord	1.85	1.39	0.70	1.71	1.30	0.65
	Rand	1.81	1.25	0.64	1.84	1.23	0.63
$Co_{1-x}Ni_x$	Ord	1.47	1.11	0.81	1.40	1.19	0.92
	Rand	1.48	1.20	0.85	1.42	1.18	0.93
$Co_{1-x}Cu_x$	Ord	1.26	0.74	0.32	1.26	0.85	0.32
	Rand	1.27	0.78	0.37	1.20	0.78	0.35
$Ni_{1-x}Cu_x$	Ord	0.24	0.00	0.00	0.33	0.14	0.01
	Rand	0.00	0.00	0.00	0.40	0.16	0.01

alloy is $0.08\mu_B$ in the theoretical data and $0.07\mu_B$ for the measurements. In the case of the ordered fcc alloys reliable experimental information can be found for the $Fe_{25}Ni_{75}$ system. Here the mean atomic moment derived from the magnitude of volume magnetization increases from $1.15\mu_B$ in the random alloy to $1.22\mu_B$ in the ordered alloy,[31] in excellent agreement with the calculated results. Also, our calculated magnetic moments for ordered FeCo and FeNi alloys are in very good agreement with numerous earlier theoretical calculations of these systems.[55,57–59,46,47]

The following trends are seen when analyzing the results presented in Table III. Firstly, the degree of order does not strongly influence the magnetic moment, except for two cases, the fcc $Fe_{75}Ni_{25}$ and the bcc $Ni_{75}Cu_{25}$ alloys which are both in the vicinity of the PM to the FM transition. This is again related to the fact that the magnetic moment of $3d$ transition-metal alloys is formed by quite localized d-electron states which are not supposed to be too sensitive to the local environment effects. Secondly, we find that almost all Fe alloys increase their magnetic moments slightly upon ordering. This fact is in agreement with the behavior of the local magnetic moment on an Fe site discussed in Sec. IV where it was shown that the Fe magnetic moment increases with increasing impurity concentration, i.e., with increasing number of unlike atoms in the first coordination shell. This is essentially the case for the ordered $B2$, $L1_0$, and $L1_2$ structures. The only exception here is the $Fe_{75}Cu_{25}$ fcc alloy which has a concentration close to the HS-LS magnetic phase transition. Using similar arguments, one expects that the magnetic moments of ordered Cu-Ni alloys on the underlying fcc lattice should decrease, and this expectation is supported by calculations. Note that all random bcc Cu-Ni alloys are paramagnetic, but the partially ordered $Ni_{75}Cu_{25}$ $B2$ alloy has a magnetic moment $\sim 0.24\mu_B$. The energy difference between the FM and the PM solution in this case, however, is ~ 1 meV, which is at the limit of the accuracy of our calculations. In case of Co alloys we have an intermediate situation: an ordering on the fcc lattice increases magnetic moment, but the average magnetic moment decreases upon ordering in the bcc alloys (except alloys with Fe).

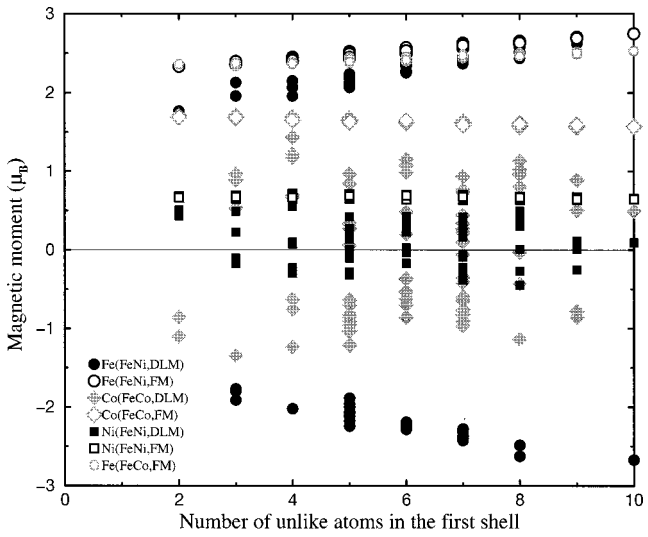

FIG. 11. Magnetic moment on one site as a function of number of unlike atoms in the first coordination shell of this site for random fcc $Fe_{50}Co_{50}$ (gray symbols) and $Fe_{50}Ni_{50}$ (black symbols) alloys, modeled by supercells with 144 atoms. The single value of the Wigner-Seitz radius $R_{WS}=2.633$ a.u. was used. Magnetic moments on Fe, Co, and Ni atoms are shown by circles, squares, and diamonds, respectively. Results of ferromagnetic (FM) calculations are given by open symbols, while calculations for disordered local moment orientations (DLM) are shown by filled symbols.

VI. INFLUENCE OF LOCAL ENVIRONMENT ON MAGNETIC MOMENTS

To explain the observed trends of the average individual magnetic moments of Fe, Co, and Ni, careful consideration of the complicated interplay between chemical and magnetic local environments of different atoms in an alloy is required (Cu has an almost filled d band, which makes it more or less nonmagnetic in all environments and no such study is motivated). This is not easily done within the mean-field approximation,[49] but can be done in the framework of the supercell approach.[25,46,50] As a matter of fact, to achieve this goal we can analyze results of our LSGF self-consistent calculations for fcc $Fe_{50}Co_{50}$ and $Fe_{50}Ni_{50}$ alloys modeled by a large supercell of 144 atoms, used in Sec. IV to illustrate the applicability of CPA to the problems considered in the present paper. Moreover, in addition to the ferromagnetic calculations we have also performed calculations for the supercell described above with a random initial distribution of the local moments, i.e., with disordered local moments (DLM). The total energy for such a supercell, when self-consistency has been obtained for the Kohn-Sham equations, is higher than for the ferromagnetic configuration by 76 meV for $Fe_{50}Co_{50}$ and by 50 meV for $Fe_{50}Ni_{50}$. Even though these solutions are only metastable, the results obtained for the DLM configurations allow a more detailed study of the dependence of the local magnetic moments of atoms on their chemical and magnetical environment.

In Figs. 11 and 12 we present calculated local magnetic moments of FeCo and FeNi alloys for different sites in the supercell plotted as a function of number of unlike nearest neighbors in their first coordination shell (i.e., local chemical environment) and as a function of the total magnetic moment in the first coordination shell (i.e., local magnetic environ-

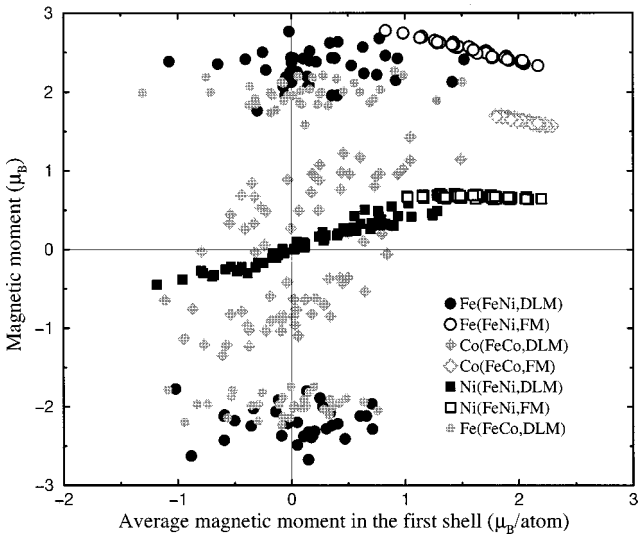

FIG. 12. Magnetic moment on one site as a function of average magnetic moment in the first coordination shell of this site for random fcc Fe_{50} Co_{50} and Fe_{50} Ni_{50} alloys. Notations are the same as in Fig. 11.

ment), respectively. Open symbols correspond to the ferromagnetic solutions (FM), while filled symbols correspond to the metastable DLM configurations. A lower magnetic moment in the first coordination shell for FM samples means that there are less Fe atoms there. For the DLM samples, on the other hand, no prediction of the number of Fe atoms can be done from the magnetic moment in the first coordination shell because the moments can have different directions.

One can see from Fig. 11 that the absolute value of the magnetic moment on an Fe atom increases linearly with increasing number of unlike nearest neighbors for both the DLM and the FM configurations. The local magnetic environment (Fig. 12) seems, however, to be uncorrelated with the magnetic moment of the Fe atom, since this atom does not seem to depend on the average moment of the first shell. In the DLM sample the magnitude and sign of the magnetic moment of Fe is uncorrelated with the magnitude and the sign of the moment in the first coordination shell. In the FM sample, the magnetic moment of Fe even decreases with increasing magnetic moment in neighborhood. For this sample, this is identical to increasing number of other Fe atoms in the neighborhood of a particular site. To conclude, the magnetic moment of Fe depends mainly on the chemical surrounding and not on the magnetical surrounding.

The opposite situation is found for Ni. The magnetic moment is independent of the chemical surrounding (see Fig. 11) but depends on the magnetical surrounding (see Fig. 12). In Fig. 12 a linear increase of the magnetic moment of the Ni atom with increasing moment on the neighboring atoms is seen for the DLM sample until saturation is reached. Notable is that Ni is nonmagnetic in a nonmagnetic surrounding. In the FM sample, the magnetic moment is constant both with respect to number of unlike atoms and magnetic moment in the first shell. This is because in FM $Fe_{50}Ni_{50}$ the surrounding is always magnetic enough to yield a saturated moment on the Ni atom.

Co exhibits a behavior that is intermediate to that of Fe and Ni. Its moment decreases slowly with an increasing number of unlike nearest neighbors and increases slowly with increasing total moment in the first shell, showing a large uncertainty in the DLM samples.

With this knowledge it is easy to explain our results for the concentration dependence of individual magnetic moments (Figs. 7–9), as well as their dependence on the degree of order. The increase of the magnetic moment of Fe when it is alloyed with other elements is a response that is typical for Fe when the number of unlike atoms increases, as seen above. For Ni the magnetic surrounding is of importance for the magnetic moment of the atom. When it is alloyed with Fe or Co, which have larger local magnetic moments than Ni, the magnetic moment remains constant (saturated). When, on the other hand, it is alloyed with Cu, which is nonmagnetic, the Ni magnetic moment drops more or less linearly with increasing amount of Cu atoms in the alloy (and, of course, in the neighborhood of the Ni atom), i.e., with decreasing average magnetic moment in its first coordination shell. The behavior of Co, as we have already mentioned, is intermediate that of Fe and Ni.

In connection with the discussion above we remark here that, at present, the most common way of investigating the temperature evolution of magnetic properties of metals and alloys is Monte Carlo simulations based on the classical Heisenberg Hamiltonian. One of the consequences of our results is an expectation that such simulations for Ni, Co, and their alloys must include the possibility for the magnitude of the magnetic moment to change. An example of this approach can be found in Refs. 51,52. The first-principles spin-dynamics simulations, of course, contain this effect automatically.[9]

VII. COMMENTS ON THE COLLINEAR SPIN MODEL

In Fig. 1 we see a few cases were experiment and theory do not agree perfectly. Mainly this is for Fe-based alloys where the high-spin to low-spin transition takes place, but also for Cu-rich fcc alloys. In the former case, theory gives sharp first-order phase transitions while experiment gives a transition that is smeared out over a small concentration interval. In the latter case we have calculated a nonzero average magnetic moment in the alloy while experiment predicts a vanishing moment. Before summing up we would like to discuss these misfits in terms of limitations of a collinear spin model.

The magnetic moment close to the HS-LS transition is very sensitive to the lattice parameter and, consequently, to intricate details of the calculations. For example, calculations based on the Korringa-Kohn-Rostoker-CPA method predict the HS to the LS transition to take place at slightly higher concentrations; about 35% of Ni in the fcc Fe-Ni[19–21,25] and about 18% of Cu in the fcc Fe-Cu.[27] However, these calculations also report the sharp first-order-type phase transition. Hence, we believe, that the main reason for the observed disagreement is the neglect of noncollinear spin configurations in the present study, as well as most other studies of magnetism in alloys.

Let us illustrate what one could expect by including the possibility of having noncollinear spin structures by considering an example of pure fcc Fe. It is now well established, theoretically, that the ground state of fcc Fe is a noncollinear antiferromagnet, and the transition from the LS to the HS

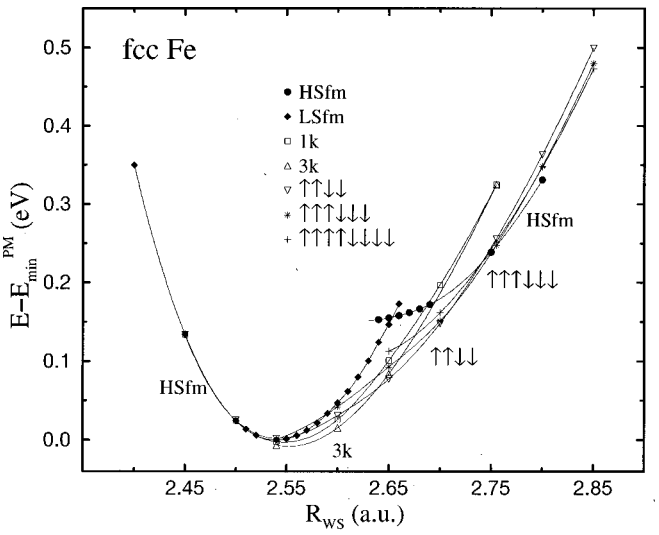

FIG. 13. Total energy of the fcc Fe (relative to the equilibrium energy of the paramagnetic fcc Fe, $E_{\min}^{\mathrm{PM}}$) as a function of Wigner-Seitz radius R_{WS} for different collinear and noncollinear spin configurations.

state goes over a series of different antiferromagnetic states.[8,7,9] In Fig. 13 we show our results for fcc Fe which include several antiferromagnetic states with collinear [$1k$, or $\uparrow\downarrow$, state along (001) direction, $\uparrow\uparrow\downarrow\downarrow$, $\uparrow\uparrow\uparrow\downarrow\downarrow\downarrow$, and $\uparrow\uparrow\uparrow\uparrow\downarrow\downarrow\downarrow\downarrow$ states along the same direction], as well as with noncollinear (the so-called $2k$ and $3k$ states) spin orientations. With this, we do not have the intention to discuss which spin configuration is the ground state for fcc Fe. Nevertheless, our results agree well with earlier studies,[9] i.e., we find that the $3k$ state with local magnetic moments $\mu = 0.98\mu_B$ has the lowest energy among all the other states considered in the present study. This state is followed by the $\uparrow\uparrow\downarrow\downarrow$ state at slightly expanded volumes. This configuration has a very strong volume dependence of the local magnetic moments (μ increases from $0.53\mu_B$ at $R_{WS}=2.54$ a.u. to $2.4\ \mu_B$ at $R_{WS}=2.755$ a.u.). In addition we find that the state with a configuration $\uparrow\uparrow\uparrow\downarrow\downarrow\downarrow$ has lower energy compared to the state with a configuration $\uparrow\uparrow\downarrow\downarrow$ at even larger volumes, but before fcc Fe becomes ferromagnetic. When this configuration is stable, the local magnetic moments which are antiparallel to each other have the magnetic moment $\mu \sim 2.3\mu_B$, while those moments which have two parallel neighbors are about $0.2\mu_B$ larger.

However, the main point we would like to emphasize in Fig. 13 is that taking noncollinear states into consideration eliminates the two-minimum structure of the binding-energy curve for fcc Fe which is obtained in conventional ferromagnetic calculations[24] and which looks similar to one presented in Fig. 3(a). Instead, this curve becomes monotonous, as indicated in Fig. 13. This effect will also take place in random alloys, and has strong impact on the study of the Invar effect. It shows that the two-state model of Weiss,[54] which, at present, is assumed in a number of models for the Invar effect[30] and which is seemingly confirmed by a number of first-principles total-energy calculations for fcc Fe, ordered Fe_3Ni structure and random fcc FeNi alloys,[40,55–59,19–21,24,25] has no solid basis. Indeed, it is unlikely that the true total-energy curve of $Fe_{56}Co_{44}$ looks like the one in Fig. 3(b), with two distinct minima. We expect that the true total energy vs volume curve is smooth and the abrupt high-spin to low-spin transition is replaced with a set of continuous transitions between different noncollinear magnetic states. The same situation is, of course, expected for fcc FeNi alloys.

As for the results presented in this paper we expect that noncollinear spin calculations for alloys would smear out the HS to the LS transition over a small concentration interval. However, we do not expect that this interval will be too wide, because the energy difference between the collinear and the noncollinear ground states in the fcc Fe is of the order of 10 meV/atom, and it is not supposed to increase greatly in alloys. On the other hand, the energy difference between the collinear HS and LS states is an order of magnitude higher and changes fast close to the concentration of the transition (see Fig. 5). Good agreement of our results with experiment at lower Fe concentrations supports this expectation.

Concerning the Cu-rich fcc alloys, we remark that, in agreement with our results, most calculations predict a nonvanishing magnetic moments on the Fe and Co impurities in Cu,[13,15,27] which also agrees with experiment. However, in a dilute alloy these moments could adopt random orientations resulting in a zero average magnetic moment.[27] Clearly, this problem, as well as noncollinear spin structure of the Fe-rich fcc alloys, require further investigations.

VIII. SUMMARY

A detailed theoretical study of magnetic properties of all binary $3d$ alloys containing the elements Fe, Co, Ni, and Cu in three close-packed structures, fcc, hcp, and bcc, is presented. The average magnetic moment is found to follow the so-called Slater-Pauling curve when plotted as a function of the filling of the alloy d band. For the Fe-based alloys in the fcc and hcp structure a low-spin to high-spin magnetic transition are found. They occur at a certain $3d$ band filling independently with what element Fe is alloyed, and we note that in this interval of electron concentration, ferromagnetic alloys are known to exhibit Invar characteristics. The individual magnetic moments, on the other hand, depend much more weakly on the concentration, and the deviations from the rigid-band behavior show up strongly. Ordering of alloys in general influence the magnetic moments only slightly. The local moments of Fe, Co, and Ni in alloys have been investigated by means of supercell calculations and we find that the Fe moment is mostly correlated with its chemical surrounding, while the Ni moment depends more on the magnetic surrounding. Finally, we present indications that the two-state model of Weiss, for explaining the Invar effect, is likely to be wrong.

ACKNOWLEDGMENTS

We are grateful to the Swedish Natural Science Research Council for financial support. The support by the Swedish Materials Consortium #9 as well as the TMR network ''Interface magnetism'' (Contract No. EMRX-CT96-0089) is acknowledged. Finally P.J. would like to express his gratitude to the Theoretical Division of Los Alamos National Laboratory, where part of this work was performed, for great hospitality.

[1] See, for example, a series *Ferromagnetic Materials*, edited by E. P. Wohlfarth and K. H. J. Buschow (North-Holland, Amsterdam, 1980-1993), Vols. 1–7.
[2] P. Hohenberg and W. Kohn, Phys. Rev. **136**, B864 (1964).
[3] W. Kohn and L. J. Sham, Phys. Rev. **140**, A1133 (1965).
[4] U. von Barth and L. Hedin, J. Phys. C **5**, 2064 (1972).
[5] J. Korringa, Physica (Amsterdam) **13**, 392 (1947); W. Kohn and N. Rostoker, Phys. Rev. **94**, 1111 (1954).
[6] O. K. Andersen, Phys. Rev. B **12**, 3060 (1975).
[7] L. Nordström and D. J. Singh, Phys. Rev. Lett. **76**, 4420 (1996).
[8] L. M. Sandratskii and P. G. Guletskii, J. Magn. Magn. Mater. **79**, 306 (1989); J. Sticht, K. H. Hölk, and J. Kübler, J. Phys.: Condens. Matter **1**, 8155 (1998); O. N. Mryasov, V. A. Gubanov, and A. I. Liechtenstein, Phys. Rev. B **45**, 12 330 (1992); M. Uhl, L. M. Sandratskii, and J. Kübler, *ibid.* **50**, 291 (1994).
[9] V. P. Antropov, M. I. Katsnelson, M. van Schilfgaarde, and B. N. Harmon, Phys. Rev. Lett. **75**, 729 (1995); V. P. Antropov, M. I. Katsnelson, B. N. Harmon, M. van Schilfgaarde, and D. Kusnezov, Phys. Rev. B **54**, 1019 (1996).
[10] C. S. Wang and A. J. Freeman, Phys. Rev. B **24**, 4364 (1981); E. Wimmer, A. J. Freeman, and H. Krakauer, *ibid.* **30**, 3113 (1984).
[11] O. Eriksson, G.W. Fernando, and R.C. Albers, Solid State Commun. **78**, 801 (1991).
[12] M. Aldén, H. L. Skriver, S. Mirbt, and B. Johansson, Phys. Rev. Lett. **69**, 2296 (1992); M. Aldén, S. Mirbt, H. L. Skriver, N. M. Rosengaard, and B. Johansson, Phys. Rev. B **46**, 6303 (1992).
[13] P. J. Braspenning, R. Zeller, A. Lodder, and P. H. Dederichs, Phys. Rev. B **29**, 703 (1984).
[14] B. Drittler, N. Stefanou, S. Blügel, R. Zeller, and P. H. Dederichs, Phys. Rev. B **40**, 8203 (1989).
[15] P. H. Dederichs, R. Zeller, H. Akai, and H. Ebert, J. Magn. Magn. Mater. **100**, 241 (1991).
[16] V. I. Anisimov, V. P. Antropov, A. I. Liechtenstein, V. A. Gubanov, and A. V. Postnikov, Phys. Rev. B **37**, 5598 (1988).
[17] O. Yu. Kontsevoi and V. A. Gubanov, Phys. Rev. B **51**, 15 125 (1995).
[18] D. D. Johnson, F. J. Pinski, and J. B. Staunton, J. Appl. Phys. **61**, 3715 (1987).
[19] D. D. Johnson, F. J. Pinski, J. B. Staunton, B. L. Gyorffy, and G. M. Stocks, in *Physical Metallurgy of Controlled Expansion Invar-Type Alloys*, edited by K. C. Russell and D. F. Smith (The Minerals, Metals & Materials Society, Warrendale, PA, 1990), p. 3; D. D. Johnson and W. A. Shelton, in *The Invar effect: A Centennial Symposium*, edited by J. Wittenauer (The Minerals, Metals & Materials Society, Warrendale, PA, 1997), p. 63.
[20] H. Akai, J. Phys.: Condens. Matter **1**, 8045 (1989).
[21] H. Akai and P. H. Dederichs, Phys. Rev. B **47**, 8739 (1993).
[22] I. Turek, J. Kudrnovský, V. Drchal, and P. Weinberger, Phys. Rev. B **49**, 3352 (1994).
[23] J. Kudrnovský, I. Turek, A. Pasturel, R. Tetot, V. Drchal, and P. Weinberger, Phys. Rev. B **50**, 9603 (1994).
[24] I. A. Abrikosov, O. Eriksson, P. Söderlind, H. L. Skriver, and B. Johansson, Phys. Rev. B **51**, 1058 (1995).
[25] M. Schröter, H. Ebert, H. Akai, P. Entel, E. Hoffmann, and G. G. Reddy, Phys. Rev. B **52**, 188 (1995).
[26] I. A. Abrikosov, P. James, O. Eriksson, P. Söderlind, A. V. Ruban, H. L. Skriver, and B. Johansson, Phys. Rev. B **54**, 3380 (1996).
[27] A. F. Tatarchenko, V. S. Stepanyuk, W. Hergert, P. Rennert, R. Zeller, and P. H. Dederichs, Phys. Rev. B **57**, 5213 (1998).
[28] F. Ducastelle, *Order and Phase Stability in Alloys* (North-Holland, Amsterdam, 1991), p. 469.
[29] C. E. Guillaume, C. R. Hebd. Seances Acad. Sci. **125**, 235 (1897).
[30] E. F. Wasserman, in *Ferromagnetic Materials*, edited by K. H. J. Buschow and E. P. Wohlfarth (North-Holland, Amsterdam, 1990), Vol. 5, p. 237.
[31] Bonnenberg, Hempel, and Wijn, in *Numerical Data and Functional Relationship in Science and Technology*, Landolt-Börnstein, New Series, edited by H. P. J. Wijn (Springer-Verlag, Berlin, 1986), Vol. III/19a; Zibold, in *Numerical Data and Functional Relationship in Science and Technology*, Landolt-Börnstein, New Series, edited by H. P. J. Wijn (Springer-Verlag, Berlin, 1986), Vol. III/19b.
[32] H. L. Skriver, *The LMTO Method* (Springer-Verlag, Berlin, 1984).
[33] O. K. Andersen, O. Jepsen, and D. Glötzel, in *Highlights of Condensed-Matter Theory*, edited by F. Bassani, F. Fumi, and M. P. Tosi (North-Holland, New York, 1985).
[34] O. K. Andersen, Z. Pawlowska, and O. Jepsen, Phys. Rev. B **34**, 5253 (1986).
[35] I. A. Abrikosov and H. L. Skriver, Phys. Rev. B **47**, 16 532 (1993).
[36] A. V. Ruban, I. A. Abrikosov, and H. L. Skriver, Phys. Rev. B **51**, 12 958 (1995).
[37] I. A. Abrikosov, A. M. N. Niklasson, S. I. Simak, B. Johansson, A. V. Ruban, and H. L. Skriver, Phys. Rev. Lett. **76**, 4203 (1996).
[38] I. A. Abrikosov, S. I. Simak, B. Johansson, A. V. Ruban, and H. L. Skriver, Phys. Rev. B **56**, 9319 (1997).
[39] S. H. Vosko, L. Wilk, and M. Nusair, Can. J. Phys. **58**, 1200 (1908).
[40] V. L. Moruzzi, Physica B **161**, 99 (1989).
[41] Y. Ueda, S. Ikeda, Y. Mori, and H. Zaman, Mater. Sci. Eng., A **217/218**, 371 (1996).
[42] V. L. Moruzzi, P. M. Marcus, K. Schwarz, and P. Mohn, Phys. Rev. B **34**, 1784 (1986).
[43] A. P. Malozemoff, A. R. Williams, and V. L. Moruzzi, Phys. Rev. B **29**, 1620 (1984).
[44] J. Friedel, Ann. Phys. (N.Y.) **1**, 257 (1976).
[45] R. H. Victora and L. M. Falicov, Phys. Rev. B **30**, 259 (1984).
[46] K. Schwarz, P. Mohn, P. Blaha, and J. Kübler, J. Phys. F **14**, 2659 (1984).
[47] R. Richter and H. Eschrig, Phys. Scr. **37**, 948 (1988); R. Richter and H. Eschrig, J. Phys. F **18**, 1813 (1988).
[48] I. A. Abrikosov and B. Johansson, Phys. Rev. B **57**, 14 164 (1998).
[49] M. F. Ling, J. B. Staunton, and D. D. Johnson, J. Phys.: Condens. Matter **7**, 1863 (1995).
[50] A. Paintner, F. Süss, and U. Krey, J. Magn. Magn. Mater. **154**, 107 (1996).
[51] M. Uhl and J. Kübler, Phys. Rev. Lett. **77**, 334 (1996).
[52] N. M. Rosengaard and B. Johansson, Phys. Rev. B **55**, 14 975 (1997).
[53] J. Tersoff and L. M. Falicov, Phys. Rev. B **25**, 4937 (1982).
[54] R. J. Weiss, Proc. Phys. Soc. London, Sect. A **82**, 281 (1963).

[55] V. L. Moruzzi, Phys. Rev. B **41**, 6939 (1990).
[56] V. L. Moruzzi, Solid State Commun. **83**, 739 (1992).
[57] P. Mohn, K. Schwarz, and D. Wagner, Phys. Rev. B **43**, 3318 (1991).
[58] P. Entel, E. Hoffmann, P. Mohn, K. Schwarz, and V. L. Moruzzi, Phys. Rev. B **47**, 8706 (1993).
[59] E. G. Moroni and T. Jarlborg, Physica B **161**, 115 (1989); E. G. Moroni and T. Jarlborg, Phys. Rev. B **41**, 9600 (1990).